We are IntechOpen, the world's leading publisher of Open Access books Built by scientists, for scientists

6,900
Open access books available

185,000
International authors and editors

200M
Downloads

Our authors are among the

154
Countries delivered to

TOP 1%
most cited scientists

12.2%
Contributors from top 500 universities



WEB OF SCIENCE™

Selection of our books indexed in the Book Citation Index in Web of Science™ Core Collection (BKCI)

Interested in publishing with us?
Contact book.department@intechopen.com

Numbers displayed above are based on latest data collected.
For more information visit www.intechopen.com



21

Fiber Optical Parametric Amplifier as Optical Signal Processor

Shunsuke Ono
Department of Electrical Engineering, Nara National College of Technology
Japan

1. Introduction

In this chapter, using numerical simulation and experimental results, the optical signal processing characteristics of Fiber-based Optical Parametric Amplifier (FOPA) using novel highly non-linear fibers (HNLFs) including Photonic Crystal Fibers (PCFs) will be described. In the last decade, to overcome the limitation of the electrical signal processing to the ultra high bit-rate optical data streams, ultrafast all-optical signal processing techniques including OTDM (Optical Time Division Multiplex), transparent wavelength conversion and all-optical sampling have been studied and proposed for over 160 Gb/s optical data streams. For those ultrafast optical processing techniques, highly-nonlinear glass fiber-based optical signal processors have been promising due to its ultrafast response time of the nonlinear effects in glass fibers and low loss characteristic to the light signals.
FOPA exploiting four-wave mixing (FWM) occurs in HNLFs has been one of those highly-nonlinear glass fiber-based all optical signal processors for ultrafast On-Off Keyed (OOK) optical signals such as Return-to-Zero (RZ) and Non-Return-to-Zero (NRZ). In recent years, with the emergences of novel glass fiber-based HNLFs with periodical microstructures including PCFs, which shows high nonlinearity using newly proposed germanium oxide silica glasses and novel heavy-metal oxide glasses, FWM-based FOPA has shortened its fiber device length drastically from tens of kilometers to tens of meters and improved its ultrafast optical signal processing characteristics remarkably. Also, with increasing application of the phase shift keyed (PSK) optical signals such as Differential Phase Shift Keying (DPSK) and Differential Quadrature Phase Shift Keying (DQPSK) in the feasibility studies of 40 Gb/s-based optical communication systems, FWM-based FOPA has attracted much more attention again to its ultrafast optical phase controllability on time scale of a few femtoseconds. In Section 2 of this chapter, we will overview the development of the highly nonlinear glass fibers and the highly-nonlinear glass fiber-based optical signal processors including FWM-based- FOPAs. Numerical model of the signal processing characteristics of FWM-based FOPA will be introduced and overview the signal processing characteristics of FWM-based FOPA with the numerically simulated parametric gain characteristics of FWM-based FOPA In Section 4, we will introduce our experimental results of the parametric gain enhancement and the ultrafast signal processing experiments using highly-nonlinear silica glass-based FOPAs with over 160 Gb/s ultrafast optical signal data streams. Practical

applications of FOPA for optical signals are discussed and we will summarizes results and suggests directions of FOPA as an ultra fast optical signal processing device in Section 5.

2. Optical Signal Processors based on Novel Glass-Based HNLFs

2.1 Fiber-Based Ultrafast Optical Signal Processors

To overcome the limitation of the electrical signal processing to the ultra high bit-rate data streams, ultrafast all-optical signal processing techniques including the Optilcal Time Domain Multiplexing (OTDM), the transparent wavelength conversion and all-optical samplings have been eagerly studied and proposed in last decades (Westlund et al., 2002; Hedekvist et al., 1997; J. Li et al., 2001; Ho et al., 2001).

In particular, fiber-based optical signal processors exploiting the nonlinear optical effects in the glass fibers such as Self Phase Modulation (SPM), Cross Phase Modulation (XPM) and Four-Wave Mixing (FWM) and Stimulated Raman Scattering (SRS) have been promising to realize the ultrafast all optical processing devices (Optical Add/Drop Multiplexer (OADM), Demultiplexer (DEMUX), Wavelength Converter (WC), Fiber Optical Parametric Amplifier (FOPA) etc.) due to its ultrafast response time and low loss characteristic.

IntechOpen

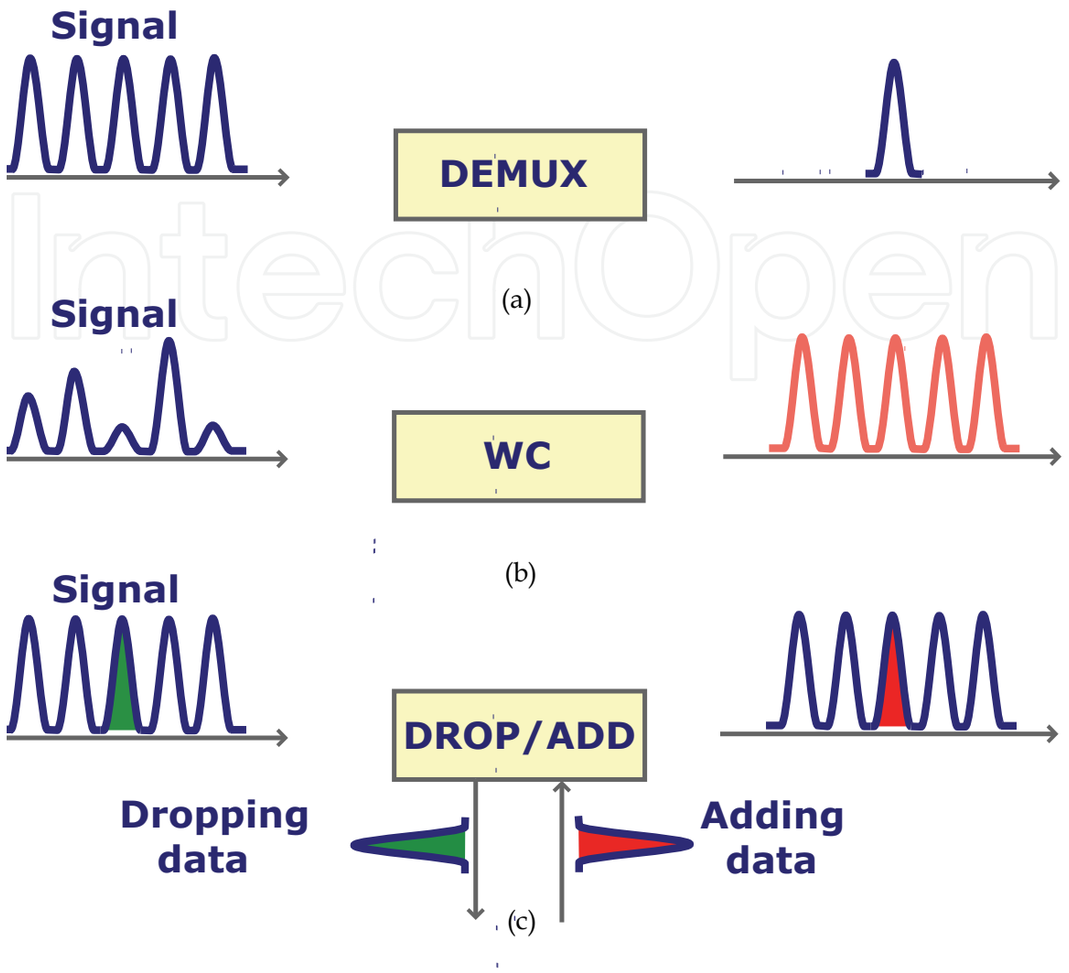


Fig. 1. Schematic diagrams of all optical ultrafast signal processors: (a) Optical DEMUX, (b) WC, and (c) OADM.

Figure 1 shows the schematic diagrams of all optical ultrafast signal processors: Optical DEMUX, WC and OADM. In particular, WC shows three active optical processings including wavelength conversion, re-amplification and re-shaping of distorted optical signals. The optical processing with re-amplification and re-shaping is usually called as optical "2R".

Generally, the nonlinear optical effects in glasses are known to occur on time scale of femto seconds (fs) which can realize the optical signal processing devices that have ultrafast response times. However, fiber-based optical signal processors have been also less realistic devices compared to other electrical signal processing devices because of their long fiber lengths. Because the fiber-based optical signal processors have been basically proposed using the silica-based glass fibers such as Dispersion Shifted Fibers (DSFs) without high nonlinearities to process the ultrafast optical signals, the fiber lengths of the silica-based nonlinear fiber devices have became very long in excess of a few hundred meters to achieve enough nonlinearities to process optical signals (Yang et al., 1997).

In general, we can obtain larger nonlinear effects in glass fibers as the fiber lengths get longer. Therefore, in order to obtain high nonlinearities, long device lengths have been required for fiber-based optical signal processors. However, such long fiber lengths have led to the relative time delay among optical signals caused by the chromatic dispersions of the fibers. As in recent commercially deployed wavelength division multiplexing (WDM) optical telecommunication systems, equally frequency-spaced many optical signal channels have been used to enhance the transmission capacities of optical transmission systems. When the fiber lengths of the fiber-based optical signal processors become longer, the chromatic dispersions of these fiber devices give rise to the relative time delay among the optical signals in WDM transmission systems, which makes it difficult to process the ultrafast optical signals allocated in wide wavelength region simultaneously.
Thus, in order to work as ultrafast optical signal processors, undesirable long device lengths have been required for fiber-based optical devices to obtain enough high nonlinearities.

2.2 Developments of Highly-Nonlinear Fibers based on Novel Glasses

In last decade, due to the development of the synthetic techniques of the novel glass materials, nonlinear characteristics of glass materials have been improved drastically and made it realize to emerge various highly-nonlinear fibers (HNLFs).
In addition, owing to the establishment of the design techniques for the spatial strong photon localization in the periodically microstructured materials and fibers based on novel highly-nonlinear glasses, Photonic Crystal Fibers (PCFs) (Birks et al., 1997), have realized extremely high nonlinearities in considerably shorter fiber lengths than those of fibers with simple core-cladding structures. The emergences of these HNLFs and PCFs fabricated by novel highly-nonlinear glass materials have given different kinds of applications for ultrafast all optical processing devices. Among these optical signal processing applications in large capacity communication networks, wavelength conversion plays a major role in providing wavelength flexibility. Therefore, in particular, WC based on FWM have been mainly proposed as a possible application for newly proposed HNLFs and PCFs in order to evaluate the optical signal processing characteristics of these HNLFs and PCFs.
On the basis of the glass fiber compositions of HNLFs and PCFs, two types of highly-nonlinear fibers have been proposed. One is the type of the glass ibers fabricated by conventional silica-based glasses and the other is the type of the glass fibers fabricated by non-silica-based glasses.
Table 1 shows the typical fiber parameters of various newly proposed silica-based and non-silica-based highly-nonlinear fibers. In particular, heavy metal oxide glass-based highly-nonlinear fibers are introduced as non-silica-based highly-nonlinear fibers.
As shown in Table 1, owing to the silica-based glass composition, silica-based highly-nonlinear fiber shows very low loss α to be 0.0005 dB/m (Onishi et al., 1997). This low loss characteristic of silica-based highly-nonlinear fiber means good compatibilities to the silica-based fibers used as transmission fibers in telecommunication systems, which leads to the low loss characteristics of silica-based highly-nonlinear fiber devices. In addition, nonlinear coefficient γ of silica-based HNLF has been reported to be ~20 $W^{-1}km^{-1}$ (Onishi et al., 1997). Silica-based HNLF realizes the high refractive index contrast between the core and clad refractive indices using germanium-doped and fluoride-doped silica glasses as the materials for the core and clad. Silica-based PCF enhances nonlinearity due to its periodical special

microstructure and achieves over three times higher nonlinear coefficient than that of the silica-based HNLF with simple core-cladding structure (Onishi et al., 1997).
Owing to the enhanced nonlinearities of silica-based HNLFs, the fiber lengths of optical signal processors using silica-based HNLFs have become much shorter than those of ones based on conventional DSFs. Also, with effectively shortening the required fiber length from kilometers to tens of meters, good optical signal processing characteristics have been evaluated for silica-based PCF using WC characteristic (Lee et al., 2003). Nevertheless, optical signal processing devices using silica-based HNLFs and PCFs still have tens of meters long fiber lengths. These rather long device lengths are much likely to bring the relative time delay among ultrafast optical signals over 160 Gb/s.

Glass composition	Structure	n^2 ($x10^{-20}m^2/W$)	γ ($W^{-1}km^{-1}$)	D@1.5 μ m (ps/nm/km)	α @1.5 μ m (dB/m)
Germanium-doped silica	Step index	~5	~20	-	0.0005
Silica	PCF	2.8	70	-30	0.19
SF57	PCF	41	640	~50	2.6
Chalcogenide	Step index	400	-	-	6.6@1.3 μ m
Bsimuth oxide	Step index	-	1100	-260	0.8
Bsimuth oxide	PCF	-	580	-9.9	1.9

Table 1. Fiber parameters of silica glass-based and non-silica glass-based highly-nonlinear fibers.

As shown in Table 1, nonlinear coefficients of the heavy metal oxide glass-based HNLFs and PCFs become nearly over ten times larger than those of silica-based HNLFs and PCFs. These enhancements of nonlinearities of heavy metal oxide glass-based HNLFs and PCFs are due to the high refractive indices of heavy metal oxide glasses. Owing to the extremely high nonlinearities of heavy metal oxide glasses, heavy metal oxide glass-based HNLFs have shortened fiber device lengths successfully from tens of meters to a few meters. In addition, using bismuth oxide glass-based HNLF, less than 1 meter-long fiber-based WC has been proposed (Lee et al., 2005) However, bismuth oxide glass-based HNLF inevitably has large material dispersion similar with other non-silica-based HNLFs fabricated by heavy metal oxide glasses, which limits the working bandwidth of WC. In general, heavy metal oxide glass-based HNLFs have been found to have extremely high nonlinearities but at the same time suffer from large group velocity dispersions (GVD), large fiber losses and large splice losses between heavy metal oxide glass-based HNLFs and conventional silica-based

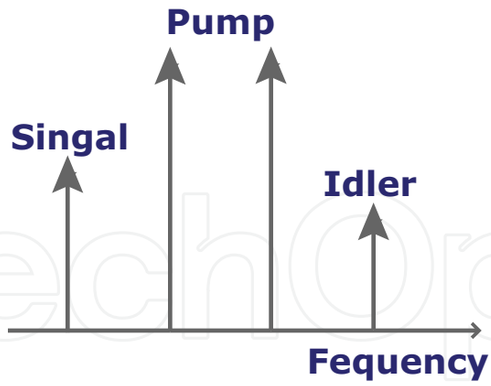
fibers. In order to obtain broadband wavelength conversion characteristics using FWM, the glass fiber used as WC should have high nonlinearity, low dispersion and low loss characteristics (Inoue et al., 1992).
Thus, in order to realize practical optical signal processing devices such as OADM, WC, DEMUX and FOPA, high nonlinearity, low dispersion, low fiber loss, low coupling loss with conventional silica-based fiber are the required fiber characteristics for silica-glass based and heavy metal oxide glass-based highly nonlinear fibers. However, at the moment, we have not obtained the highly nonlinear fiber that can satisfy all required these fiber characteristics simultaneously.

3. Optical Parametric Amplification using Four-Wave Mixing

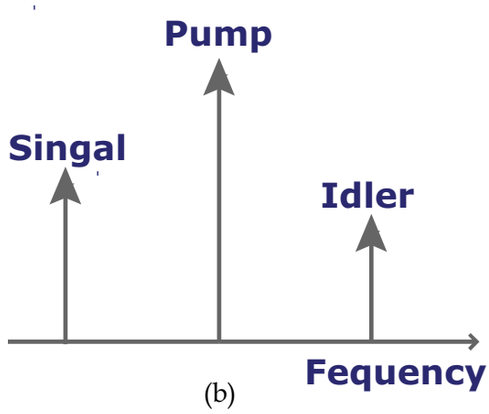
FWM has been as a main nonlinear effect to realize all optical signal processors. The optical signal processing characteristics of newly proposed HNLFs have been examined initially with the FWM efficiencies of WC using newly proposed HNLFs. Therefore, in this Section, we will introduce the precise theory of FWM and derive the coupling propagation equations of a signal, an idler and a pump light waves to establish numerical simulation model for FWM. In addition, we will overview the signal processing characteristics of FWM-based FOPA with the numerically simulated propagation characteristics of the signal along highly-nonlinear glass fibers.

3.1 Theory of Optical Parametric Amplification based on Four-Wave Mixing

As cited in Section 1 and Section 2, FWM is one of the well-known nonlinear effects occur in glass fibers similar with SPM and XPM. SPM and XPM mainly affect the phase of the pulsed optical signals due to the additional nonlinear phase shifts and cause the spectral broadening of pulsed signals, whereas FWM gives rise to the energy exchange among optical signals. Figure 2 shows the schematic diagram of FWM in the frequency domain. As shown in Figure 2, when a signal light wave and two pump light waves are input into a nonlinear glass fiber, an additional new light wave that has higher frequency than those of the two pump light waves is generated. The additional new light wave is usually called as an “idler” light.



(a)



(b)

Fig. 2. Schematic diagrams of FWMs with (a) two pump lights and (b) one pump light in the frequency domain.

When the frequencies of two pump light waves are different, the relationship among the frequencies of the signal, the two pump and the idler light waves is given by,

$$\omega_{\mathrm{i}} = \omega_{\mathrm{p1}} + \omega_{\mathrm{p2}} - \omega_{\mathrm{s}}\,, \tag{1}$$

where ω_{s}, ω_{p1}, ω_{p2} and ω_{i} are the frequencies of the signal, pumps and idler, respectively. As can be seen from Eq. (1), the energies of the signal and two pump lights are transferred to that of the idler. Therefore, FWM is usually thought to be the energy transfer phenomenon caused by the nonlinear effects in glass fibers.

When the frequencies of two pump lights are identical ($\omega_{\mathrm{p1}} = \omega_{\mathrm{p2}} = \omega_{\mathrm{p}}$), the energies of two pump lights are equally transferred to those of the signal and the idler.

Therefore, Eq. (1) becomes as follows:

$$2\omega_{\mathrm{p}} = \omega_{\mathrm{s}} + \omega_{\mathrm{l}}\,. \tag{2}$$

This case where ω_{pump1} and ω_{pump2} coincide is called as "Degenerated" Four-Wave Mixing (DFWM). In this degenerated case, the frequencies of the three waves are symmetrically

positioned relatively to each other in the frequency domain. Optical parametric amplification can be viewed from a quantum mechanical picture. Here, the degenerated parametric amplification case is manifested as the conversion of two pump photons at frequency ω_{pump} to a signal and an idler photon at frequencies ω_{signal} and ω_{idler}. The conversion needs to satisfy the energy conservation relation as in Eq. (2). From the quantum-mechanical point of view, in the degenerated case, the photon momentum conservation relation is also needed to be satisfied as follows:

$$\Delta\beta = \beta(\omega_s) + \beta(\omega_i) - 2\beta(\omega_p) = 0, \tag{3}$$

where $\beta(\omega_s)$, $\beta(\omega_i)$ and $\beta(\omega_p)$ are the wave number in vacuum, respectively and $\Delta\beta$ is the mismatch among these wave numbers. For the rest of this chapter, we will focus on the degenerated case including one pump at ω_p, one signal at ω_s and one idler light wave at ω_i. From the electromagnetic point of view, Eq. (3) is also called as "linear phase matching" condition because the wave numbers of the three light waves are directly linked to the phases of those light waves. Therefore, Eq. (3) can be considered to be the relative phase shift among the three light waves. The propagation equations of these three light waves in a transmission media are given by the following three nonlinear couple-mode equations (Agrawal., 1995):

$$\frac{dA_p}{dz} = \frac{1}{2}\alpha A_p + i\gamma\left\{ [|A_p|^2 + 2(|A_s|^2 + |A_i|^2)]A_p + 2A_s A_i A_p^* \exp(i\Delta\beta z) \right\}, \tag{4}$$

$$\frac{dA_s}{dz} = \frac{1}{2}\alpha A_s + i\gamma\left\{ [|A_s|^2 + 2(|A_i|^2 + |A_p|^2)]A_s + A_i^* A_p^2 \exp(-i\Delta\beta z) \right\}, \tag{5}$$

$$\frac{dA_i}{dz} = \frac{1}{2}\alpha A_i + i\gamma\left\{ [|A_i|^2 + 2(|A_s|^2 + |A_i|^2)]A_p + A_s^* A_p^2 \exp(-i\Delta\beta z) \right\}. \tag{6}$$

where A_s A_i and A_p are the complex field amplitude of the signal, the idler and pump light waves, respectively. z is the longitudinal coordinate along the fiber as the transmission media. α is the loss of the glass fiber for these three light waves. $\gamma = 2\pi n_2 / A_{\text{eff}}$ is the nonlinear coefficient of the fiber where n_2 is the nonlinear parameter and A_{eff} is the effective modal area of the fiber. In Eq. (4), Eq. (5) and Eq. (6), the first two terms are responsible for the nonlinear phase shift caused by SPM and XPM, respectively. The last terms of these couple-mode equations contribute to the energy transfer among the signal, the idler and the pump light waves.

Furthermore, to obtain further understanding to the propagation characteristics of the three light waves in the fiber, Eq. (4), Eq. (5) and Eq. (6) are rewritten by using $A_j = P_j^{1/2}\exp(i\phi_j)$ (j=s, i, p) where P_j (j=s, i, p) is the power of the three light waves and ϕ_j (j=s, i, p) is the phases of the these light waves, respectively. Thus, we can obtain practical propagating equations to describe the propagation characteristics of the signal, the idler and the pump lights as follows:

$$\frac{dP_p}{dz} = \alpha P_p - 4\gamma[(P_s P_i P_p^2)^{1/2}\sin\theta], \tag{7}$$

$$\frac{dP_s}{dz} = \alpha P_s + 2\gamma[(P_s P_i P_p^2)^{1/2} \sin\theta], \quad (8)$$

$$\frac{dP_i}{dz} = \alpha P_i + 2\gamma[(P_s P_i P_p^2)^{1/2} \sin\theta], \quad (9)$$

$$\frac{d\theta}{dz} = \Delta\beta + \gamma(2P_p - P_s - P_i) + \gamma[(P_P^2 P_i / P_s)^{1/2} + (P_P^2 P_s / P_i)^{1/2} - 4(P_s P_i)^{1/2}]\cos\theta . \quad (10)$$

Here, Eq. 10 describes the propagation characteristics of the relative phase among three light waves. The first term of Eq. 10 is the contribution from the linear phase shift that does not depend on the powers of three light waves. The second and third term of Eq. 10 show the contributions from the nonlinear phase shifts caused by the nonlinearity of the glass fiber.
To simulate the frequency dependence of the optical amplification characteristics based on FWM, we will expand the linear phase shift $\Delta\beta$ in Taylor series to the fourth order around the zero-dispersion frequency ω_0. Thus, we can obtain the frequency-dependent linear phase shift $\Delta\beta$ given by,

$$\Delta\beta = \left\{ \beta_3(\omega_p - \omega_0) + \frac{\beta_4}{2}[(\omega_p - \omega_0)^2 + \frac{1}{6}(\omega_p - \omega_s)^2] \right\}(\omega_p - \omega_s)^2 . \quad (11)$$

Here, β_3 and β_4 is the third and fourth order dispersions defined at ω_0. Also, β_2 (the second order dispersion of $\beta(\omega)$) becomes zero because $\beta_2(\omega_0) = 0$. Usually, β_2 and β_3 are called as "dispersion" and "dispersion slope" of the fiber, respectively. In addition, when the pump frequency ω_p is chosen to become $\omega_p = \omega_0$, the frequency dependent part of $\Delta\beta$ is fully dominated by the fourth-order dispersion β_4. Therefore, the gain bandwidth of FOPA is strongly limited by the fourth-order dispersion β_4 (Marhic et al., 1996). To realize the broad band optical signal wavelength converter using FOPA based on FWM, the value of β_4 has been improved in silica-based highly nonlinear glass fibers (Hirano et al., 2005). Higher order dispersions become an important limiting factor as the optical signal operating bandwidth $\Delta\lambda = |\lambda_p - \lambda_s|$ exceeds 100 nm.

3.2 Numerical Analysis on Gain Characteristics of FWM-based FOPA

Next, using the simulation model based on the reduced propagation equations (7), (8), (9) & (10), we will overview the signal processing characteristics of FWM-based FOPA with the numerically simulated parametric gain characteristics of FWM-based FOPA. In this numerical simulation, we used further reduced Eq. (12) and Eq. (13) obtained by neglecting β_4 and by assuming that FOPA are operated in a phase-matching condition that the relative phase remains near π/2 in Eq. (10) and Eq. (11). Eq. (12) and Eq. (13) are given by;,

$$\kappa = \Delta\beta + 2\gamma(P_p - P_s - P_i) , \quad (12)$$

$$\Delta\beta = -\frac{2\pi c\lambda_0^3}{\lambda_P^3 \lambda_S^2}\frac{dD_C}{d\lambda}(\lambda_P - \lambda_S)^2(\lambda_P - \lambda_0) , \quad (13)$$

where κ and $\Delta\beta$ show the linear and total phase mismatch parameters, respectively. γ is the nonlinear coefficient of HNLF. P_j (j=s, p, i) and λ_j (j=s, p, i) show the powers and wavelengths of signal, pump and idler, respectively. $dD/d\lambda_c$ is the dispersion slope at the

zero dispersion wavelength of HNLF. It is known that the parametric gain of FWM-based FOPA shows the maximum value when FWM-based FOPA is operated in the total phase-matching condition $\kappa = 0$ is satisfied.

As shown in Eq. (12), the total phase mismatch consists of the linear phase mismatch part $\Delta\beta$ and the nonlinear phase mismatch part $2\gamma(P_p - P_s - P_i)$. The linear phase mismatch part $\Delta\beta$ does not depend on the powers of signal, pump and idler. Therefore, $\Delta\beta$ becomes the constant phase mismatch factor for FOPA. On the other hand, the nonlinear phase mismatch part $2\gamma(P_p - P_s - P_i)$ apparently depends on the powers of signal, pump and idler. Therefore, when the powers of signal, pump and idler are varied in FWM-based FOPA, parametric gain characteristics of FWM-based FOPA are affected sensitively by the total phase mismatching due to the variation of these powers.

Firstly, we will overview this parametric gain variation of FWM-based FOPA induced by the input power with the gain characteristics of FWM-based FOPA with different pump powers shown in Figure 3.

Table 2 shows the fiber parameters of silica-based HNLF used in this analysis on the parametric gain characteristics of FWM-based FOPA. In this numerical simulation, the parametric gain media of FOPA is assumed to be a germanium-doped silica-based HNLF with nonlinear coefficient 25 $W^{-1}Km^{-1}$ and 150 m of the fiber length. Then, the pump wavelength is set to be 1562 nm longer than zero dispersion wavelength of the fiber 1555.5 nm. The input signal power into HNLF is -30 dBm. As shown in Figure 3, the parametric gain of FOPA becomes to show two symmetrical peaks about the pump wavelength as the higher pump power input into HNLF. At the wavelengths where the parametric gain shows its peaks, total phase-matching condition $\kappa = 0$ is fully satisfied. Whereas the parametric gain shows peaked gain shape with high pump power (P_p = 30 dBm), almost flat parametric gain shape is obtained with low pump power (P_p = 20 dBm). This pump power dependence of the parametric gain characteristics shows that the difference in the parametric gain evolution rates is induced by the power-dependent nonlinear phase mismatch part $2\gamma(P_p - P_s - P_i)$. Generally, it is known that the parametric gain characteristics are exponentially proportional to the applied pump power in the wavelength region where the perfect phase-matching condition $\kappa = 0$ is satisfied. Also, the parametric gain characteristics are quadratically proportional to the applied pump power in the wavelength region where the linear phase-matching condition $\Delta\beta = 0$ is satisfied. Figure 4 shows the simulated parametric gain evolutions of a signal and an idler along the silica-based HNLF with two different wavelengths. One is 1540 nm where the total phase-matching condition $\kappa = 0$ is found to be almost satisfied show in Figure 3. The other is 1560.5 nm near the pump wavelength 1562 nm where the linear phase-matching condition $\Delta\beta = 0$ is satisfied.

As shown in Figure 4, the difference between parametric gains at 1540 nm and 1560.5 nm becomes larger as the signal propagation distance gets longer. This implies that the fiber length should be shortened to obtain the flat parametric gain shape of FOPA. On the other hand, long fiber length is required to obtain large parametric gain of FOPA. Thus, it is difficult to realize large and flat gain characteristics of FOPA simultaneously. So far, in order to achieve large and flat gain characteristics of FOPA, the gain enhancement schemes of FOPA with broad gain characteristics have been proposed. Therefore, in Section 4, in order to realize the FOPA with large and flat gain characteristics, we will propose a novel parametric gain enhancement scheme of FOPA with flat gain characteristics.

Simulation parameters of HNLF	
Glass composition	Germanium SiO_2
Fiber length [m]	150
Nonlinear coefficient [$W^{-1}km^{-1}$]	25
Zero dispersion wavelength [nm]	1555.5
Dispersion Slope [$ps/nm/km^2$]	0.03
Fiber loss [dB/km]	0.5

Table 2. Fiber parameters of silica-based HNLF.

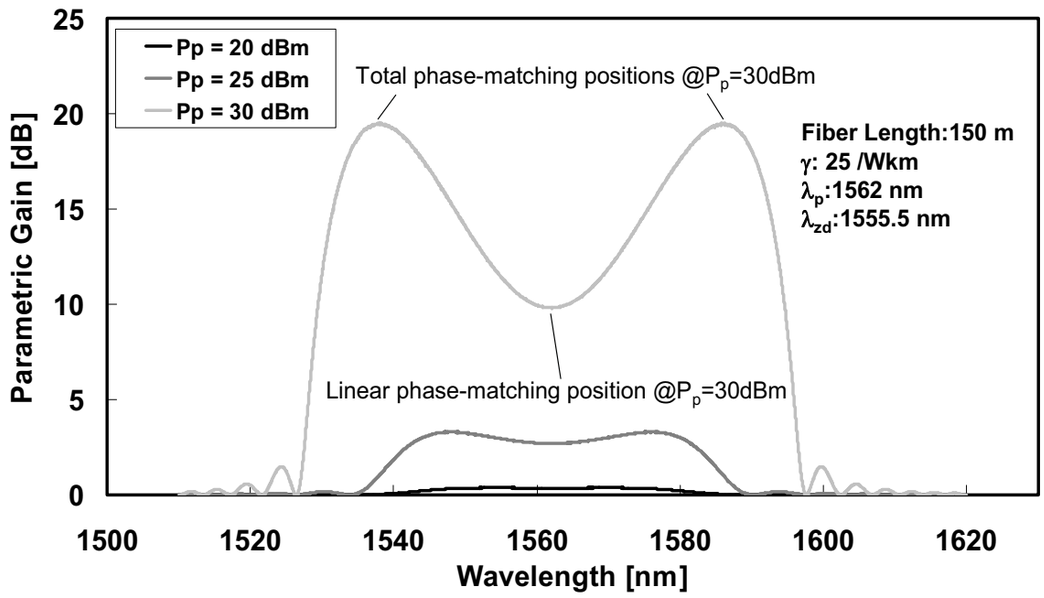


Fig. 3. Simulated parametric gain characteristics of silica glass-based FOPA with various pump powers (P_p = 10 dBm , 20 dBm and 30 dBm).

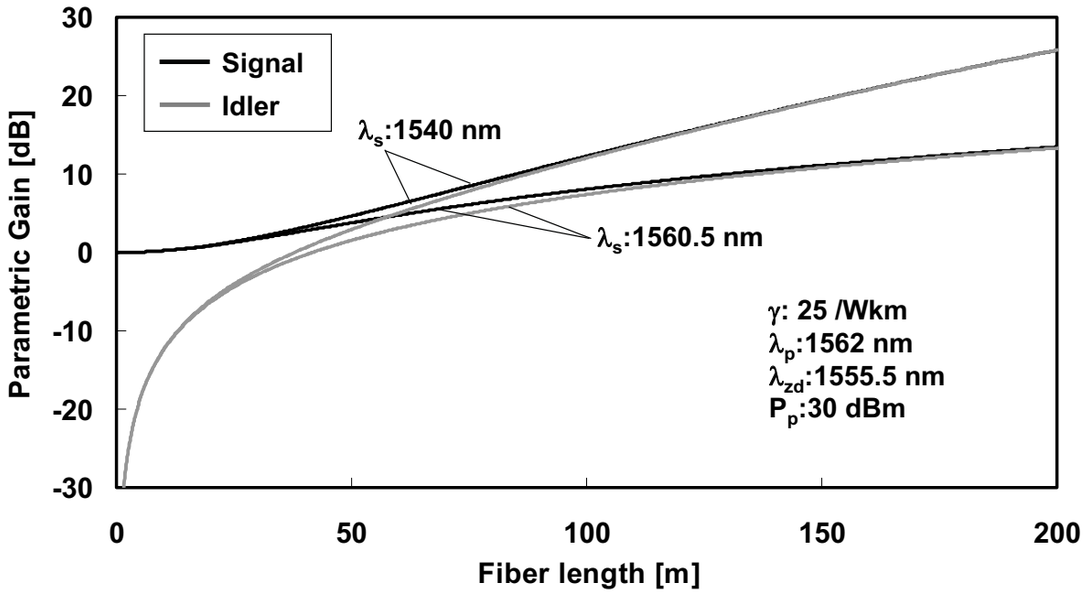


Fig. 4. Fiber propagation characteristics of the parametric gains of signals and idlers with different wavelengths (λ_s = 1540 nm and 1560.5 nm).

4. Application of FOPA to Ultrafast Optical Signal Processing Device

In this Section, we will introduce our experimental results of the ultrafast signal processing experiments using single-pumped FOPAs as an broadband ultrafast optical DEMUX with large parametric gain characteristics for over 160 Gb/s optical signal data streams. On the basis of our proposed design schemes for FOPA, we performed evaluations on the parametric gain characteristics of the single-pumped cascaded silica-glass-based HNLFs with different dispersions and dispersion slopes.

As results of this evaluation, it was shown that over 20 dB parametric gains can be achieved in ~ 50 nm band width in C-band wavelength region. Apparent improvement in the parametric gain characteristics was observed in the wavelength region near the pump wavelength. Furthermore, to verify the capability of our proposed FOPA as an ultrafast optical signal processor, we performed transparent 160 Gb/s – 10 Gb/s DEMUX experiments using 160 Gb/s On-Off keyed (OOK) data using the parametric gain-enhanced FOPA by our proposed design scheme. As a result, no error penalty occurred for 160 Gb/s ultrafast data streams in the transparent 160 Gb/s – 10 Gb/s DEMUX experiment.

4.1 Broadband FOPA Design Scheme with Perfect Phase-matching Condition

So far, FOPA and Nonlinear Loop Mirror (NOLM) have been proposed as all optical fiber-based DEMUX. In principle, the optical gating action controlled by optical clock pulses is required for optical DEMUX. Figure 5 shows the comparison of the optical DEMUX characteristics of NOLM-based DEMUX and FOPA-based DEMUX.

As shown in Figure 5, NOLM-based DEMUX cannot amplify the input signal and can bring the interference between incoming and counter propagate pulse. For ultrafast optical fast

signals, this interference between incoming and counter propagate pulse can deteriorate the optical data streams in NOLM-based DEMUX. On the other hand, FOPA based DEMUX can amplify the incoming data signal with parametric gain. Also, there is no interference of data pulses in FOPA-based DEMUX. Therefore, in this work, we used FOPA as optical DEMUX for ultrafast optical signal processing. The results of transparent 160 Gb/s – 10 Gb/s DEMUX experiments using FOPA-based ultrafast DEMUX are will be shown in Section 4.

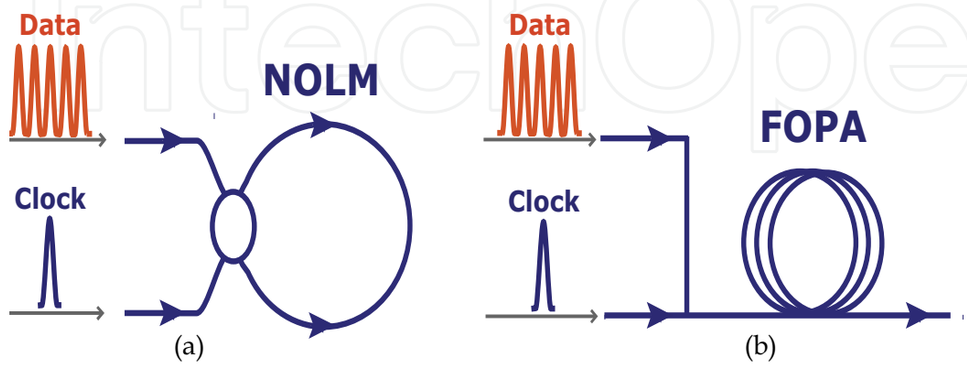


Fig. 5. Schematic diagrams of the principles of the optical gating operations in (a) NOLM and (b) FOPA.

In order to realize the broadband ultrafast optical DEMUX using FOPA, large FOPA gain characteristics in a wide wavelength region should be realized. So far, in order to achieve large and broad gain characteristics of FOPA, the gain enhancement schemes of FOPA with broad gain characteristics have been proposed using many cascaded HNLFs with dual pump scheme. However, using many HNLFs and dual pump scheme is not suitable way to realize the practical FOPA for optical signal processors because of the complicated HNLF's configuration and the use of two pump lasers, which leads to the increase of splice losses between HNLFs and the less cost effectiveness. Particularly, in order to realize an optical DEMUX using FOPA, the optical gating of the optical DEMUX should be controlled by single pump light source as an optical clock pulse because it is extremely difficult to adjust and control the relative timing among ultrafast optical signals over 160 Gb/s and multi-pump light pulses. In order to realize a practical FOPA with large and broad parametric gain characteristics using single pump light source, simpler design scheme of FOPA are required. Therefore, we propose a simple and practical design scheme to achieve large and broad parametric gain characteristics of FOPA exploiting the perfect phase-matching condition of FWM.

Figure 6 shows the optical parametric gain characteristics of FOPA achieved in the perfect-matched and linear phase-matching conditions. When the perfect phase-matching condition $\kappa = \Delta\beta + 2\gamma(P_p - P_s - P_i) = 0$ is achieved, the parametric gain shows the exponential characteristics in terms of the pump power as shown in Section 3. In addition, if the linear phase-matching condition $\Delta\beta = 0$ is only satisfied, the parametric gain characteristics becomes quadratic one. In our design scheme, we particularly tried to improve the gain characteristics in the wavelength region near the pump wavelength because the gain depletion occurs significantly in that wavelength region.

Figure 7 shows the schematic design concept of the switching gain band width enhancement using quasi-cascaded two HNLFs with different dispersions and dispersion slopes. The term "quasi" is used because there is not much difference between the optical parameters of these two HNLFs. In this two HNLFs configuration scheme, the zero dispersion wavelength of 1st HNLF is set to become slightly shorter than the pump wavelength, which makes the wavelength of the parametric gain peak relatively far from the pump wavelength. Also, the zero dispersion wavelength of 2nd HNLF is set to become shorter than that of the 1st HNLF in order to make the wavelength of the gain peak of 2nd HNLF longer. In addition, the dispersion slope of the 2nd HNLF is set to be relatively steeper than that of 1st HNLF to make the maximum gain peak of the 2nd HNLF shift toward the pump wavelength in the shorter wavelength. With this design scheme, the improvement of the parametric gain characteristics particularly in the wavelength region near the pump wavelength can be expected.

4.2 Experimental Setup

4.2.1 Evaluations of Optical Parametric Gain Characteristics of FOPA

Figure 8 shows the experimental configuration for the parametric gain characteristic evaluation. The proposed design scheme for HNLFs to achieve high and broadened parametric switching gains was tested using a quasi-cascaded HNLF consists of two HNLFs.

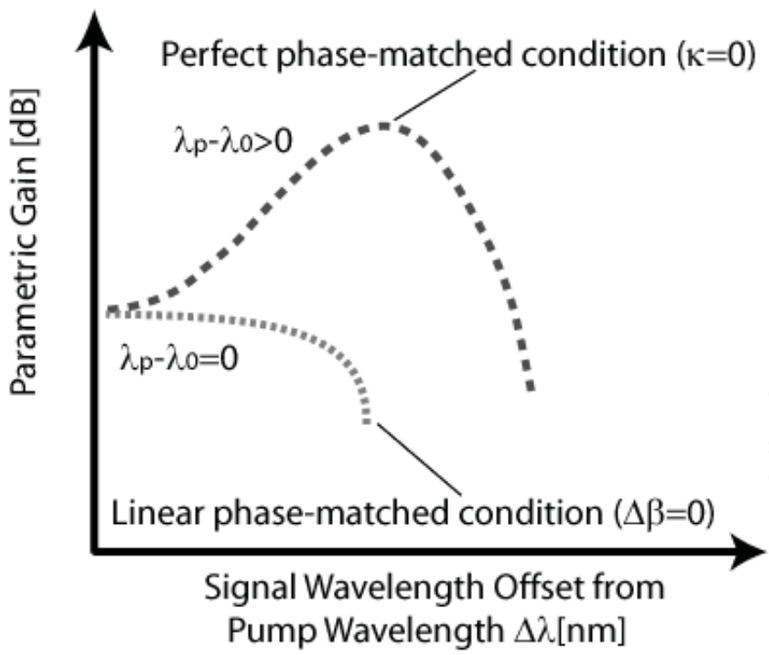


Fig. 6. Schematic diagrams of the optical parametric gain characteristics of FOPA achieved in the perfect-matched ($\kappa = 0$) and the linear phase-matching conditions ($\Delta\beta = 0$).

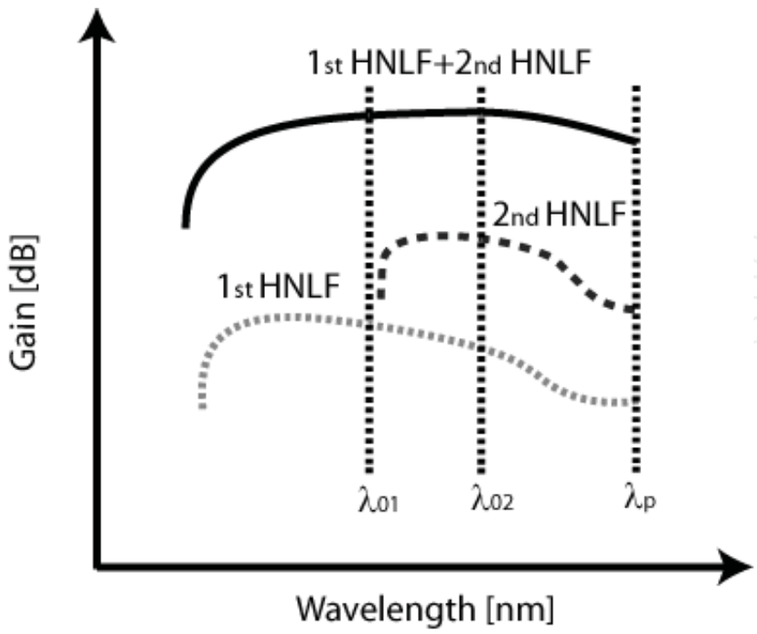


Fig. 7. Schematic diagram of the design concept for the parametric gain bandwidth enhancement using the quasi-cascaded two HNLFs with different dispersions and dispersion slopes.

Two HNLFs have the zero dispersion slopes and the zero dispersion wavelengths (λ_{01}, $dD/d\lambda_{01}$) = (1570 nm, 0.03 ps/nm^2/km) and (λ_{02}, $dD/d\lambda_2$) = (1555 nm, 0.035 ps/nm^2/km), respectively. The nonlinear coefficients γ of the HNLFs are ~21 W^{-1}km^{-1}. A modelocked Fiber laser (MLFL) as a signal source generated a 10 GHz optical pulse train at wavelengths in the wavelength region from 1520 nm to 1550 nm. A tunable laser source was used as pump source, which was modulated by an Electro-Absorbtive (EA) modulator and a $LiNbO_3$ intensity modulator (LN, 10 Gb/s, PRBS: 2^{23}-1) to realize the wide pulse width with the repetition rate 311MHz and a high peak power at the fiber input. Maximum pump peak power was about 43 dBm. A signal was input to the quasi-cascaded HNLFs together with a pump pulse that had ~45 degree-aligned polarization to that of the signal pulse. The wavelength of the pump pulse was 1570.5 nm to have almost the same wavelength of the 1st HNLF. The pulse widths (FWHM) of the signal and control pulses were 1.6 ps and 25 ps, respectively.

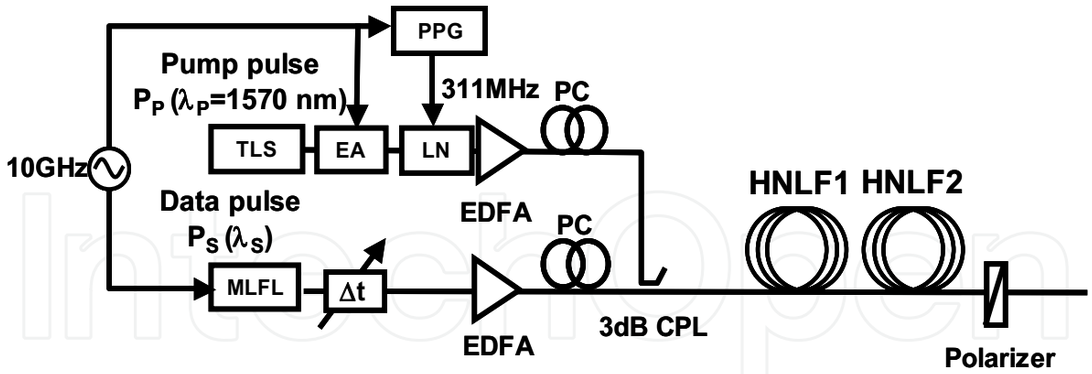


Fig. 8. Schematic diagram of the experimental setup for the evaluation on the parametric gain characteristic of proposed quasi-cascaded HNLFs.

4.2.2 160 Gb/s -10 Gb/s DEXUM Experiment using Quasi-Cascaded HNLFs

Furthermore, we evaluated the signal processing characteristics of the perfect phase-matching FOPA using ultrafast pulse trains. 160 Gb/s – 10 Gb/s OTDM DEMUX experiment was performed using another modelocked fiber laser, which generates 1.6 ps light pulse with the pulse repetition rate 10 GH/z at the wavelength λ_s = ~1540 nm where the parametric gain characteristics improved by our proposed FOPA design scheme. This 10 Gb/s pulse was optically time-division multiplexed to generate a single polarized 160 Gb/s data pulse train. Using this pulse train as a signal, we performed 160 Gb/s – 10 Gb/s OTDM DEMUX experiments to verify the capability of the proposed FOPA as an ultrafast optical signal processor.

4.3 Results

4.3.1 Parametric Gain Characteristic of Quasi-Cascaded HNLFs

Figure 9 shows the parametric signal gain characteristics of 1st, 2nd and 1st + 2nd HNLFs. As shown in Figure 9, parametric signal gain characteristics of 1st and 2nd HNLF show the parametric gain peaks at the wavelengths ~1520 nm and ~1550 nm where phase-matching conditions $\kappa = 0$ in 1st and 2nd HNLF are satisfied. Parametric signal gain characteristic of quasi-cascaded HNLFs (1st + 2nd HNLFs) is also shown in Figure 8. As shown in Figure 8, with our proposed design concept for FOPA, parametric signal gain characteristic of cascaded HNLFs becomes flat shape compared to those of 1st and 2nd HNLF. As results of this evaluation, it was shown that over ~20 dB parametric gains can be achieved in ~ 50 nm bandwidth (from 1510 nm to 1560 nm) in C-band wavelength region. In particular, improvement in the parametric gain characteristics was observed in the wavelength region near the pump wavelength 1570 nm.

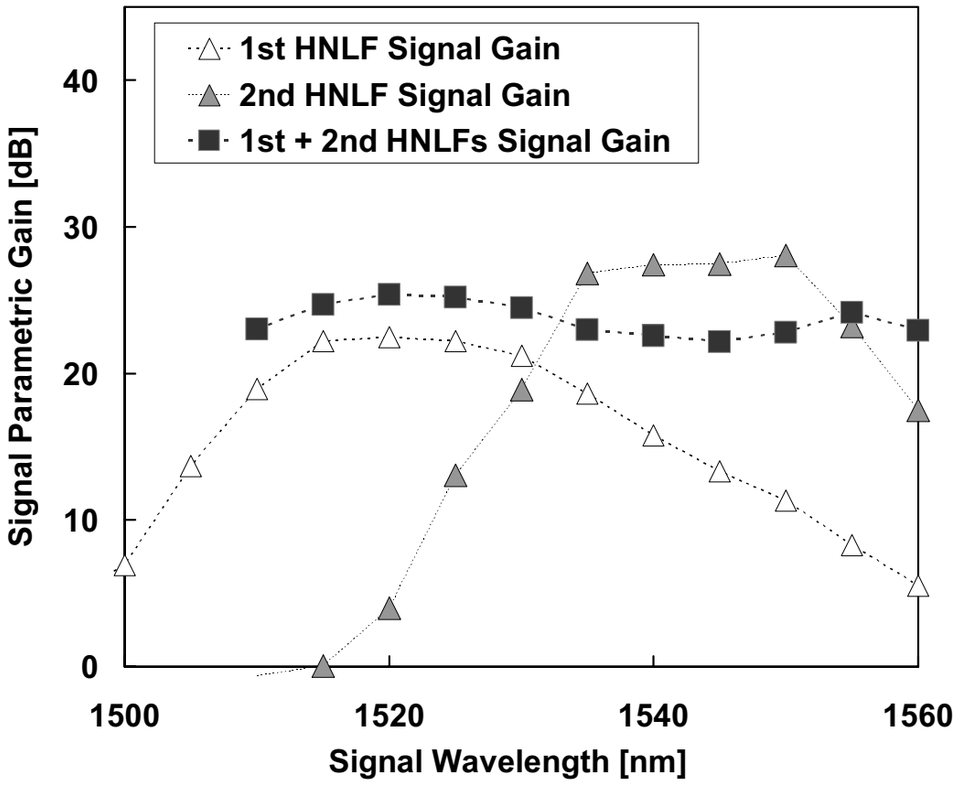


Fig. 9. Parametric gain characteristics of 1st HNLF, 2nd HNLF and 1st + 2nd HNLFs.

4.3.2 High Speed Switching Characteristics in 160 Gb/s – 10 Gb/s DEMUX

Figure 10 shows the measured bit error rates (BERs) obtained by 160 Gb/s - 10 Gb/s OTDM DEMUX experiments. The eye-patterns in the BER measurements of 10 Gb/s reference and 160 Gb/s - 10 Gb/s OTDM DEMUX are also shown (inset (a) and inset (b)). As shown in Figure 10, error free operations were demonstrated successfully without wavelength conversion for the OTDM DEMUXs of 160 Gb/s pulse trains. No penalty was occurred in the 160 Gb/s – 10 Gb/s transparent OTDM experiment compared to the 10 Gb/s reference BER curve. Therefore, No degradations of demuxed 10 Gb/s signal pulses occur after optical signal processing using our proposed FOPA-based optical demultiplexer. Also, compared to the input 160 Gb/s pulse trains, DEMUXed 10 Gb/s signal pulses show over 20 dB pulse gain induced by a perfect phase-matching. As results of 160 Gb/s - 10 Gb/s OTDM DEMUX experiments, our proposed FOPA is considered to be work as optical DEMUX with large parametric gain for up to 160 Gb/s ultrafast optical data streams.

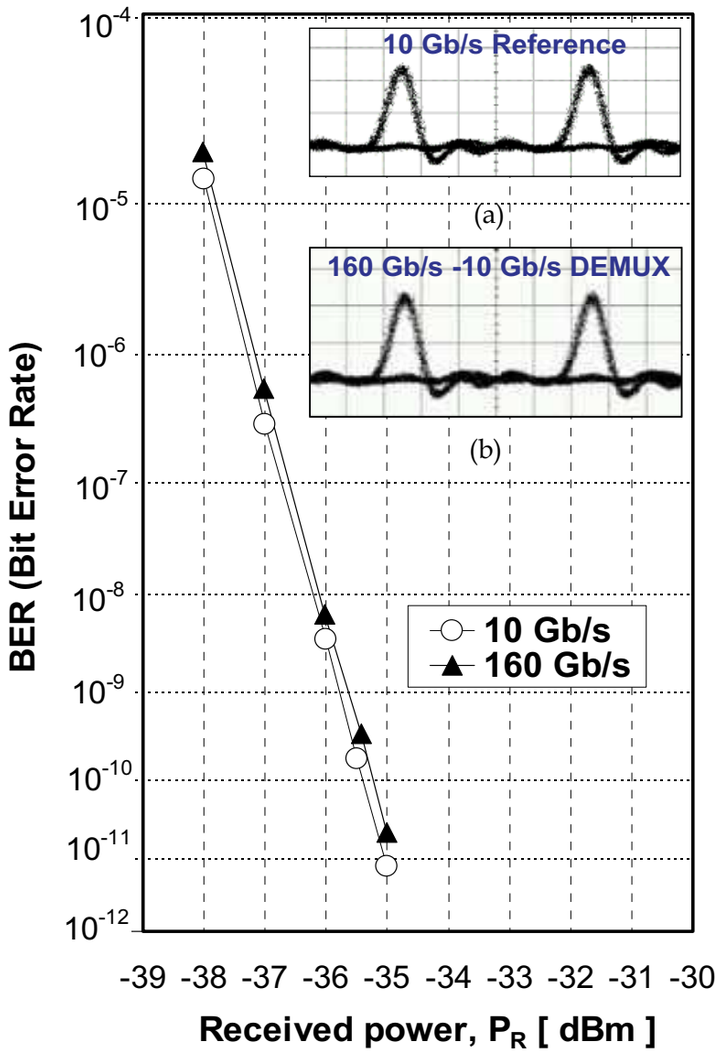


Fig. 10. Bit error rates (BERs) obtained by 160 Gb/s - 10 Gb/s OTDM DEMUX experiments. The eye-patterns in the BER measurements of 10 Gb/s reference (inset (a)) and 160 Gb/s - 10 Gb/s OTDM DEMUX (inset (b)) are also shown.

5. Conclusion

In this chapter, we overviewed the developments of highly-nonlinear glass materials and the optical signal processing functions of highly-nonlinear glass-based FOPA. The parametric gain characteristics of highly-nonlinear glass based FOPA in phase-matching conditions were introduced using numerical simulations based on FWM coupling equations. Using the parametric gain characteristics of FOPA in perfect phase-matching condition, in order to realize a practical glass-fiber based FOPA, we proposed the simple and practical design scheme to achieve the broad and large parametric gain characteristics of FOPA using silica glass-based HNLF and single pump As a result, with proposed FOPA design scheme,

over 20 dB parametric gain was achieved in 50 nm band width in the C-band wavelength region. In particular, apparent improvement in the parametric gain characteristics was observed in the wavelength region near the pump wavelength. Furthermore, we performed 160 Gb/s – 10 Gb/s OTDM DEMUX experiments at the wavelength where the parametric gain characteristics improved. In the ultrafast DEMUX experiments, we verified that no error penalty occurred for 160 Gb/s pulse trains. This result shows that our design scheme for FOPA using the perfect phase-matching condition of FWM is effective for the transparent DEMUX of the ultra high bit-rate pulses over 160 Gb/s.

6. References

Agrawal, G. P. (1995). Nonlinear Fiber Optics, 2nd edition, Academic express, San Diego, CA, USA.

Aso, O.; Arai, S.; Yagi, T.; Tadakuma, M.; Suzuki, Y. & Namiki, S. (2000). Broadband four-wave mixing generation in short optical fibers, Electron. Lett. Vol. 36, pp. 709 - 711.

Asobe, M.; Kanamori, T. & Kubodera, K. (1993). Applications of highly nonlinear chalcogenide glass fibers in ultrafast all-optical switches, IEEE Journal of Quantum Electronics. Vol. 29, pp. 2325-2333.

Birks, T.A.; Knight, J.C. & St. J. Russell, P. (1997) Endlessly single-mode photonic crystal fiber, Optics Letters, Vol. 22, No 13, pp. 961-963.

Chow, K. K.; Kikuchi, K.; Nagashima, T.; Hasegawa, T.; Ohara, S. & Sugimoto, N. (2007). Four-wave mixing based widely tunable wavelength conversion using 1-m dispersion-shifted bismuth-oxide photonic crystal fiber, Optics Express Vol. 15, pp. 15418-15423.

Hedekvist, P. O.; Karlsson, M. & Andrekson, P. A. (1997). Fiber four-wave mixing demultiplexing with inherent parametric amplification, J. Lightwave Technol., vol.15, pp. 2051 – 2058.

Hirano, M.; Nakanishi, T.; Okuno, T. & Onishi, M. (2005). Broadband Wavelength Conversion over 193-nm by HNL-DSF Improving Higher-order Dispersion Performance, ECOC 2005 Proceedings, Vol. 6, pp. 43-44.

Ho, M. C.; Uesaka, K.; Marhic, M. E.; Akasaka, Y. & Kazovsky, L. G. (2001). 200-nm-bandwidth fiber optical amplifier combining parametric and raman gain, Journal of Lightwave Technology, vol.19, pp. 977 – 981.

Inoue, K. & Toba, H. (1992). Wavelength conversion experiment using fiber four-wave mixing, IEEE Photonics Technology Letters, Vol. 4, pp. 69-72.

Lee, J. H.; Belardi, W.; Furusawa, K.; Petropoulos, P.; Yusoff, Z.; Monro, T.M.; & Richardson, D.J. (2003). Four-wave mixing based 10 Gbit/s tunable wavelength conversion using a holey fiber with a high SBS threshold, IEEE Photonics Technology Letters, Vol.15, pp. 440-442.

Lee, J. H.; Nagashima, T.; Hasegawa, T.; Ohara, S.; Sugimoto, N. & Kikuchi, K. (2005). Four-wave- mixing-based wavelength conversion of 40-Gb/s nonreturn-to-zero signal using 40-cm bismuth oxide nonlinear optical fiber, IEEE Photonics Technology Lettes, Vol.17, no.7, pp. 1474-1476.

Li, J.; Hansryd, J.; Hedekvist, P. O.; Andrekson, P. A. & Knudsen, S. N. (2001). 300Gbit/s eye-diagram measurement by optical sampling using fiber and Exhibit, Optical Fiber Communication Conference, March 17-22, Anaheim, CA.

Marhic, M. E.; Kagi, N.; Chiang, T.-K. & Kazovsky, L. G. (1996). Broadband fiber optical parametric amplifiers, Optics Express, Vol. 21, pp. 573–575.

Onishi, M.; Okuno, M.; Kashiwada, T.; Ishikawa, T. ; Akaska, S. & Nishimura, N. (1997). Integrated Optics and Optical Fiber Communications, 11th International Conference on, and 23rd European Conference on Optical Communications, Vol. 2, pp. 115 – 118.

Petropoulos, P.; Ebendorff-Heidepriem,Heike.; Finazzi, V.; Moore, R.; Frampton, K.; Richardson, D. & Monro, T. (2003). Highly nonlinear and anomalously dispersive lead silicate glass holey fibers, Optics Express Vol.11, pp. 3568-3573.

Yang, F. S.; Ho, M. C.; Marhic, M. E. & Kazovsky, L. G. (1997). Demonstration of two-pump fiber optical parametric amplification, Lasers and Electro-Optics Society Annual Meeting 1997, LEOS '97 10th Annual Meeting. Vol. 1.

Westlund, M.; Hansryd, J.; Andrekson, P. A. & Knudsen, S. N. (2002). Trans-parent wavelength conversion in fiber with 24nm pump tuning range, Electron. Lett., vol.38, pp. 85 – 86.

IntechOpen



Optical Fiber New Developments

Edited by Christophe Lethien

ISBN 978-953-7619-50-3

Hard cover, 586 pages

Publisher InTech

Published online 01, December, 2009

Published in print edition December, 2009

The optical fibre technology is one of the hop topics developed in the beginning of the 21th century and could substantially benefit applications dealing with lighting, sensing and communication systems. Many improvements have been made in the past years to reduce the fibre attenuation and to improve the fibre performance. Nowadays, new applications have been developed over the scientific community and this book fits this paradigm. It summarizes the current status of know-how in optical fibre applications and represents a further source of information dealing with two main topics: the development of fibre optics sensors, and the application of optical fibre for telecommunication systems.

How to reference

In order to correctly reference this scholarly work, feel free to copy and paste the following:

Shunsuke Ono (2009). Fiber Optical Parametric Amplifier as Optical Signal Processor, Optical Fiber New Developments, Christophe Lethien (Ed.), ISBN: 978-953-7619-50-3, InTech, Available from: http://www.intechopen.com/books/optical-fiber-new-developments/fiber-optical-parametric-amplifier-as-optical-signal-processor

INTECH
open science | open minds

InTech Europe
University Campus STeP Ri
Slavka Krautzeka 83/A
51000 Rijeka, Croatia
Phone: +385 (51) 770 447
Fax: +385 (51) 686 166
www.intechopen.com

InTech China
Unit 405, Office Block, Hotel Equatorial Shanghai
No.65, Yan An Road (West), Shanghai, 200040, China
中国上海市延安西路65号上海国际贵都大饭店办公楼405单元
Phone: +86-21-62489820
Fax: +86-21-62489821

© 2009 The Author(s). Licensee IntechOpen. This chapter is distributed under the terms of the Creative Commons Attribution-NonCommercial-ShareAlike-3.0 License, which permits use, distribution and reproduction for non-commercial purposes, provided the original is properly cited and derivative works building on this content are distributed under the same license.

IntechOpen

IntechOpen